

# An IR study of methanol steam reforming over ex-hydrotalcite Cu–Zn–Al catalysts

M.A. Larrubia Vargas<sup>a,1</sup>, G. Busca<sup>a,\*</sup>, U. Costantino<sup>b</sup>, F. Marmottini<sup>b</sup>,  
T. Montanari<sup>a</sup>, P. Patrono<sup>c</sup>, F. Pinzari<sup>c</sup>, G. Ramis<sup>a</sup>

<sup>a</sup> Dipartimento di Ingegneria Chimica e di Processo, Università di Genova, P.le J.F. Kennedy, I-16129 Genova, Italy

<sup>b</sup> CEMIN, Centro di Eccellenza sui Materiali Innovativi Nanostrutturati, Dipartimento di Chimica, Università di Perugia, I-06100 Perugia, Italy

<sup>c</sup> Istituto di Metodologie Inorganiche e dei Plasmi, CNR, Via Salaria Km. 29,300, I-00016 Roma, Italy

Received 6 July 2006; received in revised form 21 August 2006; accepted 29 August 2006

Available online 5 September 2006

## Abstract

A Cu–ZnO–Al<sub>2</sub>O<sub>3</sub> catalyst prepared via hydrotalcite-like hydroxycarbonate precursor, has been tested in the oxidative steam reforming of methanol (MOSR) to produce hydrogen and CO<sub>2</sub> with poor CO content in a flow reactor. The conversion of methanol over oxidized, reduced and hydrated catalyst has been investigated by IR spectroscopy. The reactions of CO over hydrated and reduced surfaces and of the CO<sub>2</sub> + H<sub>2</sub> mixture has also been investigated by IR in the range 200–400 °C.

It has been concluded that during methanol steam reforming the catalyst works in a partially oxidized state. Methoxy and formate groups are intermediates in the reaction. The key step for low CO concentration in the products is the fast oxidation of adsorbed CO to CO<sub>2</sub>. Pure methanol decomposition to CO and hydrogen, instead, occurs over highly reduced catalyst. The mechanism of the water gas shift reaction has also been discussed.

© 2006 Elsevier B.V. All rights reserved.

**Keywords:** Methanol steam reforming; Hydrogen production; Reaction mechanism; IR spectroscopy; Methanol decomposition and synthesis; Water gas shift; Cu–Zn–Al catalysts

## 1. Introduction

Catalysts belonging to the Cu–ZnO–Al<sub>2</sub>O<sub>3</sub> system have been applied for the synthesis of methanol from syngas promoted by the presence of CO<sub>2</sub> [1,2] since ICI introduced the low temperature methanol synthesis technology in 1966 [3]:



Catalysts belonging to the same system have also been applied since many years for the low temperature water gas shift reaction (WGS) [2,4]:

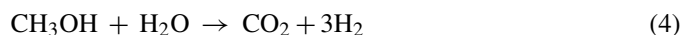


to convert CO to CO<sub>2</sub> while further producing H<sub>2</sub> in processes such as pure hydrogen production and ammonia synthesis, usually starting from methane steam reforming.

Hydrogen can also be produced by methanol simple decomposition (i.e. the reverse of methanol synthesis)



or by methanol steam reforming (MSR),



so that methanol shows potentiality as an “hydrogen vector”. More than 10 medium-size plants (100–1000 Nm<sup>3</sup>/h) are in operation worldwide for the stationary production of hydrogen from methanol for chemical and electronic industry with the Tøpsoe “package hydrogen plants” [5,6]. Methanol and water vapour are fed into a multitubular reactor heated externally by a hot oil circulation. Although the Tøpsoe process is reported to be “based on methanol decomposition”, the published data suggest that the reaction mostly occurs through MSR. Cu–ZnO–Al<sub>2</sub>O<sub>3</sub>

\* Corresponding author. Tel.: +39 0103536024; fax: +39 0103536028.  
E-mail address: [Guido.Busca@unige.it](mailto:Guido.Busca@unige.it) (G. Busca).

<sup>1</sup> On leave from Departamento de Ingenieria Quimica, Universidad de Malaga, Spain.

catalysts, prepared by coprecipitation, via malachite-boehmite intermediates [7,8], are very likely applied for this process.

In the scientific literature, the most frequently tested catalysts for MSR and oxidative MSR (i.e. the coupling of methanol selective oxidation and steam reforming) belong to this system with quite an high copper content (30–50%, wt/wt as CuO). The commercially available industrial low temperature WGS catalysts are mostly tested for MSR and MOSR [9–12] although they have been optimized for WGS.

In recent papers we found that Cu–ZnO–Al<sub>2</sub>O<sub>3</sub> catalysts obtained by decomposition of hydrotalcite-type precursors, having the formula [Cu<sub>y</sub>Zn<sub>1-x-y</sub>Al<sub>x</sub>(OH)<sub>2</sub>](CO<sub>3</sub>)<sub>x/2</sub>(1–3x/2)H<sub>2</sub>O are active in methanol decomposition, MSR and OMSR even at low Cu content [13–15].

The mechanisms of these reactions over Cu–ZnO–Al<sub>2</sub>O<sub>3</sub> catalysts are still incompletely defined. The mechanism of the WGS equilibrium over these catalysts, either adsorptive through formate ions or regenerative through a redox cycle of copper centers, is still under debate [4,16]. According to Chinchén and Spencer [17] the actual reactant for methanol synthesis is CO<sub>2</sub>. The reaction should occur through formation of formates and their hydrogenolysis to methoxy groups. Just the reverse should occur for methanol decomposition. Some authors suppose MSR to be due to a sequence of methanol decomposition (producing CO) and WGS (converting CO into CO<sub>2</sub>) [18]. Other authors, however, provided evidence that CO<sub>2</sub> may be the primary product under steam reforming conditions, and that CO is likely produced from CO<sub>2</sub> by the reverse WGS reaction [13–15,19–21]. It has been concluded that the rate determining step in both methanol decomposition (giving rise to CO and hydrogen) and methanol steam reforming (producing CO<sub>2</sub> and hydrogen) is the same, i.e. the dehydrogenation of adsorbed methoxy groups [22]. However, the nature of the selectivity determining step allowing the production of CO<sub>2</sub> under steam reforming conditions is still far from clear. Additionally, the role of oxidized copper ions, assumed to be active in methanol synthesis [23], as well as the activating role of Zn oxide [24] are still not defined.

In this paper we re-investigated the surface chemistry of a low-Cu-content Cu–Zn–Al catalyst through IR spectroscopy. The aim is to have further insight on the mechanism of the mentioned reactions.

## 2. Experimental

Details on the preparation of the hydrotalcite precursor, with Cu:Zn:Al ratios 5:52:43, have been reported elsewhere [25]. Its phase purity (XRD, Philips PW 100) is 100% hydrotalcite-type, its surface area is 63 m<sup>2</sup>/g obtained with the BET method from N<sub>2</sub> adsorption isotherms at 77 K (Micromeritics 2010). After calcination in air for 2 h at 450 °C the surface area is 149 m<sup>2</sup>/g.

The catalytic activity measurements were performed in a fixed-bed flow microreactor using 45 mg of catalyst diluted with  $\alpha$ -Al<sub>2</sub>O<sub>3</sub> powder in 1:10 ratio in order to obtain isothermal condition. In each experiment, the catalyst was pre-treated with

100 cm<sup>3</sup>/min of 5% O<sub>2</sub> in helium for 2 h, and later reduced with 5% of H<sub>2</sub> in He at 450 °C.

The MOSR tests were performed at atmospheric pressure feeding the reactor (i.d. 1 cm with a coaxial centered thermocouple with its tip located in the middle of the catalytic bed) with 16.11% CH<sub>3</sub>OH, CH<sub>3</sub>OH/H<sub>2</sub>O/O<sub>2</sub> molar ratios 1/1.1/0.12, He balance, at  $\tau=0.03$  g cm<sup>-3</sup> s contact time. Helium was used as carrier gas. The methanol and water liquid mixture was fed using a pump Sage Instruments Model 341 A.

The catalytic reaction products were analyzed on-line by a Carlo Erba GC equipped with a TCD detector and an Hayesep D column for the separation of H<sub>2</sub>, CO<sub>2</sub>, CH<sub>3</sub>OH, H<sub>2</sub>O, DME at 130 °C and O<sub>2</sub> and CO when column was kept to 30 °C. Product gas composition was calculated from the concentration and flow rates of the gas stream excluding He used for the dilution.

The IR spectra were recorded with a Nicolet Nexus Fourier Transform instrument. A conventional manipulation/outgassing ramp connected to the IR cell was used. For the analysis of the skeletal vibrations KBr pressed disks were used. For adsorption experiments pressed disks of pure catalyst powders (15 mg, 2 cm diameter) were used. The samples were thermally pre-treated in the IR cell by heating in air at 450 °C for 2 h and later reduced in pure H<sub>2</sub> two cycles with 400 Torr for 30 min each time. The adsorption procedure involves contact of the activated sample disk with CO at –140 °C in the conventional IR cell cooled with liquid nitrogen. Desorption is carried out by outgassing upon warming from –140 °C to room temperature.

## 3. Results and discussion

### 3.1. Catalyst structure

XRD and IR spectra show that the fresh catalyst is a poorly crystallized spinel-type phase mixed oxide. After catalytic tests the features of the hydrotalcite-like hydroxycarbonate precursor reappear confirming the well known memory effect of these materials [26].

### 3.2. Catalytic activity in the oxidative steam reforming of methanol

The catalytic activity is very weak in our conditions at 250 and 300 °C (conversion of methanol <3%). The catalytic activity becomes significant for  $\tau=0.03$  g cm<sup>-3</sup> s at 350 °C, methanol conversion being above 90% at 400 °C and total at 450 °C. Hydrogen yield (Fig. 1, left) grows in parallel until near 2.7 mol<sub>H<sub>2</sub></sub>/mol<sub>CH<sub>3</sub>OH</sub> fed at 450 °C. The only detected carbon containing products are CO<sub>2</sub>, largely predominant, and CO: no traces of organic compounds (e.g. formaldehyde, dimethylether, methylformate, formic acid) have been found under these conditions. The conversion to CO (CO yield, curves on the right) increases with reaction temperature but does not exceed 0.75% at 450 °C. The ratio CO/CO<sub>2</sub> is much lower than expected from thermodynamics showing that the WGS reaction is far from equilibrium.

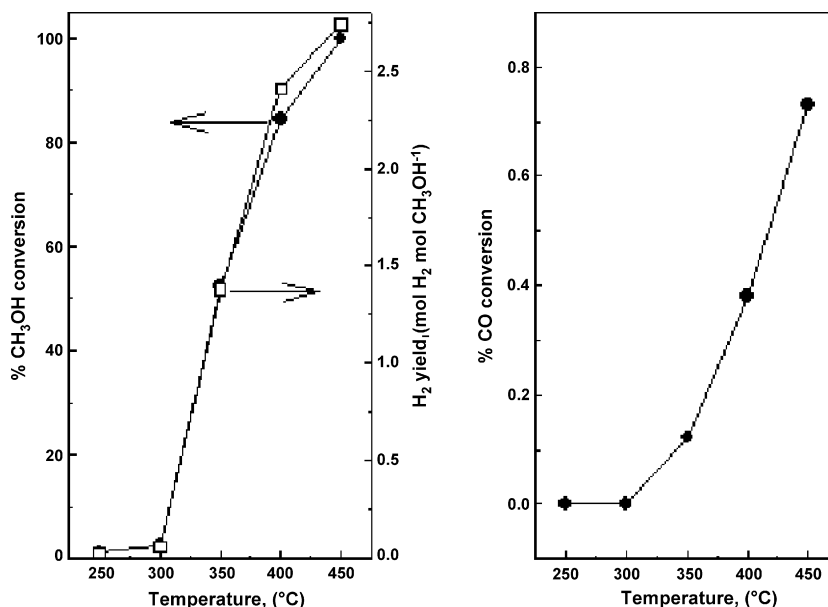


Fig. 1. Methanol conversion, hydrogen yield and conversion to CO vs. reaction temperatures on the catalyst calcined at 450 °C at  $\tau = 0.03 \text{ g cm}^{-3} \text{ s}$ .

### 3.3. IR study of the catalyst reduction

In Fig. 2 the spectra of a disk of the catalyst is reported after two different pretreatments. Spectrum (a) has been recorded after outgassing at 450 °C, while spectrum (b) has been recorded after reduction in hydrogen at 450 °C and outgassing at 450 °C. The difference spectrum reported in the inset in Fig. 2 shows that reduction causes a partial growth of the sample's absorption mainly due to a broad band centered more or less near 2000  $\text{cm}^{-1}$ . We previously found [15] that this absorption becomes stronger by increasing copper content in reduced samples. So we attribute this absorption to copper metal particles. Additionally, the bands due to carbonates residual from the preparation method, found at 1550 and 1395  $\text{cm}^{-1}$  on the simply outgassed sample, decrease a little bit in intensity while the intensity of the band at 2341  $\text{cm}^{-1}$ , due to trapped CO<sub>2</sub> molecules, increases a little. Finally, adsorbed or trapped water, likely pro-

duced by reduction of copper in hydrogen, is also observed (stretching broad band at 3500–3000  $\text{cm}^{-1}$ , sharp bending band at 1625  $\text{cm}^{-1}$ ). An extremely weak feature at 2180  $\text{cm}^{-1}$ , likely due to trapped CO, can also be found. The band observed at 1030  $\text{cm}^{-1}$ , resembles that previously found on Cu–Zn–Cr catalysts and attributed, according to H/D isotopic exchange experiments, to vibrations involving adsorbed hydrogen species [27], which persist after outgassing at 250 °C.

### 3.4. IR study of water adsorption on the reduced catalyst

In Fig. 3 the spectra relative to the adsorption of water on the prerduced catalyst are shown. In the presence of water vapour strong bands due to liquid-like water layers are observed (OH stretching at 3470  $\text{cm}^{-1}$ , bending at 1645  $\text{cm}^{-1}$ ). The strong bands at 1110 and 1010  $\text{cm}^{-1}$  are likely due in part to the librational modes associated to water adsorbed overlayers, that are likely also responsible for the broad band centered at 2100  $\text{cm}^{-1}$ .

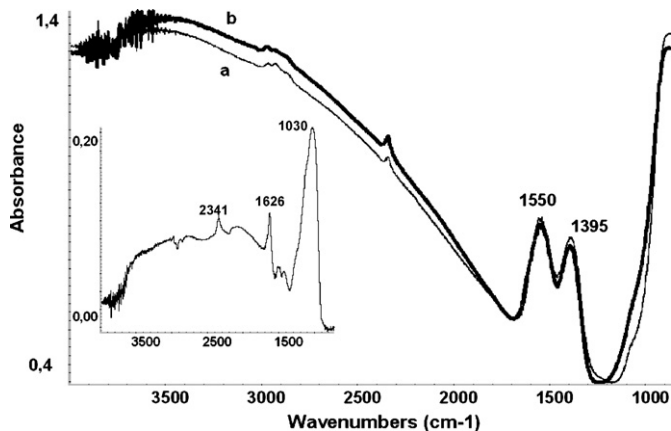


Fig. 2. FT-IR spectra of the catalyst after simple outgassing at 450 °C (a) and after previous reduction in hydrogen at 450 °C and outgassing at 450 °C (b). In the inset b – a subtraction spectrum.

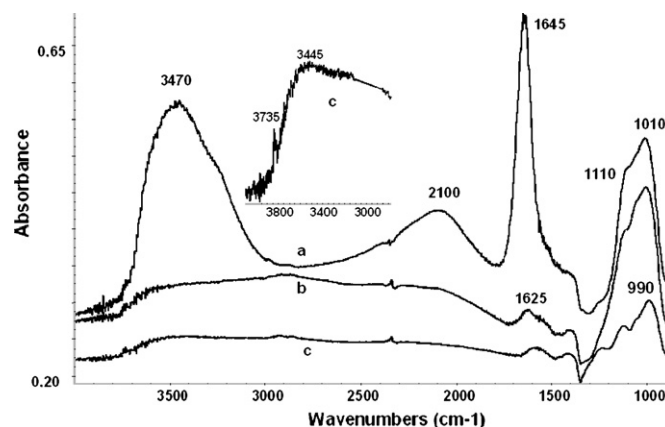


Fig. 3. FT-IR spectra of the adsorbed species formed after hydration of the catalyst pre-reduced at 450 °C (a), after evacuation at r.t. (b) and at 200 °C (c).

Outgassing at r.t. causes the almost complete disappearance of molecular water. Outgassing at 200 °C leaves a broad adsorption in the region 3700–3000  $\text{cm}^{-1}$  where a sharp peak is observed near 3735  $\text{cm}^{-1}$  with a broad maximum at 3445  $\text{cm}^{-1}$ . These features may be due to OH stretchings of free and H-bonded hydroxyl groups, respectively. Together, some perturbation occurs in the region of carbonates (1600–1300  $\text{cm}^{-1}$ ), and a strong absorption persists at 990  $\text{cm}^{-1}$  with shoulders at 1120 and 1230  $\text{cm}^{-1}$ , possibly associated to OH out of plane deformations or to metal–oxygen modes. This experiment shows that adsorption of water on the prereduced catalyst mostly gives rise to surface hydroxylation.

### 3.5. IR study of methanol adsorption and conversion

In Fig. 4 the FT-IR spectra relative to the adsorption of methanol at 250 °C on the catalyst outgassed at 450 °C without any reduction treatment (except outgassing in vacuum) are reported.

In the low-frequency side of the spectrum a complex band with two main maxima at 1030 and 1081  $\text{cm}^{-1}$  is observed, with an additional component at 1190  $\text{cm}^{-1}$ . These features can be assigned to adsorbed methoxy groups. The multiplicity of the band in the region 1200–900  $\text{cm}^{-1}$ , mostly due to the C–O stretching, is due, very likely, to the presence of two or more kinds of methoxy groups. As for comparison, we can note that the C–O stretching of methoxy groups on  $\gamma\text{-Al}_2\text{O}_3$  is found at 1095  $\text{cm}^{-1}$  [28], and those on ZnO and ZnO-based systems [29] at 1060  $\text{cm}^{-1}$ . Methoxy groups on CuO are reported to be very labile, whose C–O stretching is found at 1070  $\text{cm}^{-1}$ , and finally, those on Cu(111) [30] absorb at 1036  $\text{cm}^{-1}$ . The complex weak band centered in the region 1470–1440  $\text{cm}^{-1}$  (maximum at 1458  $\text{cm}^{-1}$ ), and the component at 1190  $\text{cm}^{-1}$  are most likely due to the bending and rocking modes, respectively, of the  $\text{CH}_3$  of the methoxy groups. The relative intensity of the C–O stretching components do not seem to change very much with Cu:Zn:Al ratio in different catalysts. This makes unlikely

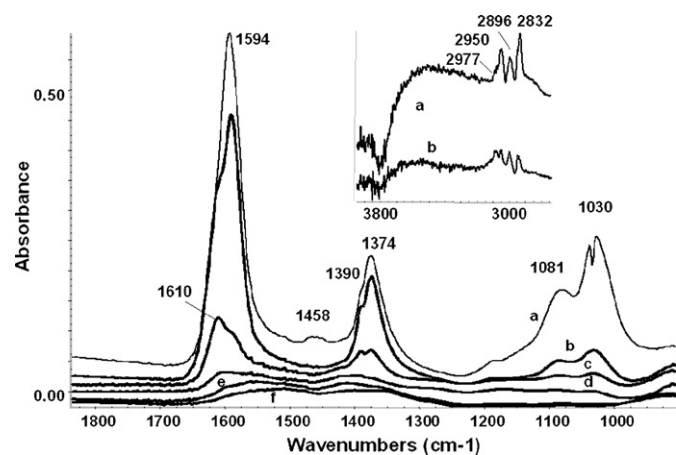


Fig. 4. FT-IR spectra of the adsorbed species formed upon adsorption on the catalyst, previously outgassed at 450 °C, of methanol 10 Torr at 250 °C; in contact with the vapour (a) and after outgassing at 250 °C (b), 300 °C (c), 350 °C (d), 400 °C (e), and 450 °C (f).

the possible assignment of species to Cu-methoxides, Zn- and Al-methoxides. On the contrary, we believe that different cations may participate to the overall coordination of methoxide groups.

The sharp strong bands at 1594  $\text{cm}^{-1}$  (having an evident component at 1610  $\text{cm}^{-1}$ ), at 1390  $\text{cm}^{-1}$  (shoulder), and 1374  $\text{cm}^{-1}$ , are typical of formate ions [31]: they are assigned to asymmetric stretching of the O–C–O group (ca. 1600  $\text{cm}^{-1}$ ), the CH deformation mode (1390  $\text{cm}^{-1}$ ), and finally, to the symmetric O–C–O stretching (1374  $\text{cm}^{-1}$ ). The splitting of the COO asymmetric stretching, with two components which behave differently upon heating, shows that two different kinds of formate groups exist. We believe that different cations may participate to the overall coordination also of formates, which are very likely bridging. For this reason it is unlikely the real existence of Cu-, Zn- and/or Al-formates.

In the CH stretching region, three weak sharp maxima at 2950, 2896 and 2830  $\text{cm}^{-1}$  and a component at 2977  $\text{cm}^{-1}$ , are found: they are due to CH stretchings of formate (2896  $\text{cm}^{-1}$ , CH stretching, 2977  $\text{cm}^{-1}$ , combination) and methoxy groups (2950 and 2830  $\text{cm}^{-1}$ ). Weak bands due to surface carbonates are also formed (ca. 1500 and 1400  $\text{cm}^{-1}$ ).

The evolution under heating shows that methoxy groups mostly disappear upon outgassing at 250 °C. Formate species characterized by the asymmetric COO band at 1610  $\text{cm}^{-1}$  (mostly decomposing above 300 °C) are more stable than those characterized by the same mode at 1594  $\text{cm}^{-1}$  (mostly decomposing between 250 and 300 °C). Part of carbonates disappear at 450 °C. The analysis of the gas phase evolved in the steps shows that upon outgassing at 250 °C methanol and  $\text{CO}_2$  mostly evolve. During thermal treatment at 300 °C  $\text{CO}_2$  mostly evolve while at higher temperatures CO mostly evolve.

In Fig. 5 the results are reported of a similar experiment performed on the catalyst after reduction in hydrogen. The intensity of the spectra of the adsorbed species formed under these conditions is much smaller (nearly one-tenth) than in the case of the unreduced catalyst. The features of two kinds of formate species (with the asymmetric stretching component split at 1621 and 1595  $\text{cm}^{-1}$ , and the symmetric stretching at 1377  $\text{cm}^{-1}$ )

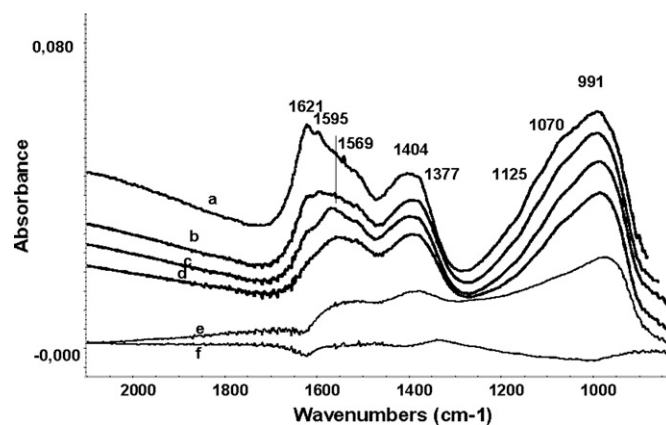


Fig. 5. FT-IR spectra of the adsorbed species formed upon adsorption on the catalyst, previously reduced in hydrogen at 450 °C and outgassed at 450 °C, of methanol 10 Torr at 250 °C; in contact with the vapour (a) and after outgassing at 250 °C (b), 300 °C (c), 350 °C (d), 400 °C (e), and 450 °C (f).



are evident but weak, together with those of carbonates ( $1569$ ,  $1404\text{ cm}^{-1}$ ). The behavior of the bands of formates is similar to that above described for the unreduced catalyst: they disappear in the range  $250$ – $350\text{ }^{\circ}\text{C}$ . The relatively stronger band at  $990\text{ cm}^{-1}$ , with several components at higher frequencies, might be due to CO stretchings of different kinds of methoxy groups. This band decreases in intensity above  $350\text{ }^{\circ}\text{C}$  down to disappear at  $450\text{ }^{\circ}\text{C}$ , i.e. well later than those of methoxy groups on the unreduced catalyst. These data can be correlated with the experiments concerning methanol steam reforming and methanol decomposition over similar catalysts [13]. In the absence of steam, methanol decomposition occurs above  $350\text{ }^{\circ}\text{C}$ . This suggests that the band at  $990\text{ cm}^{-1}$  is due to methoxy groups that decompose to CO. The lower frequency for the CO stretching of such methoxy groups, with respect to those observed on the oxidized catalyst, might be due to the bond of the former ones to Cu metal particles. Formate and carbonate species are probably mostly located over the “support” alumina–ZnO phase or on unreduced centers and may not participate to the main methanol decomposition reaction over the reduced catalyst.

The same experiment has been repeated, but after contact of the reduced catalyst with water (Fig. 6). The results of this experiment are very similar to those for the unreduced sample (Fig. 4). This suggests that the adsorption of water in the range  $30$ – $250\text{ }^{\circ}\text{C}$  substantially reoxidizes the surface. This enhances the amount of methanol adsorbed, forming methoxy and formate species, which are in fact detected much stronger in the spectra. On the other hand, the evolution of methoxy and formates is much faster on the rehydrated sample, occurring already at  $250\text{ }^{\circ}\text{C}$ , in agreement with the activity in methanol steam reforming starting in the same temperature range.

These data provide evidence for the sequence methoxy–formate–carbon oxides for the methanol steam reforming reaction. It is clear that the decomposition step of formate ions is the key for selective steam reforming of methanol (giving rise to  $\text{CO}_2$ ) versus methanol decomposition (giving rise to CO).

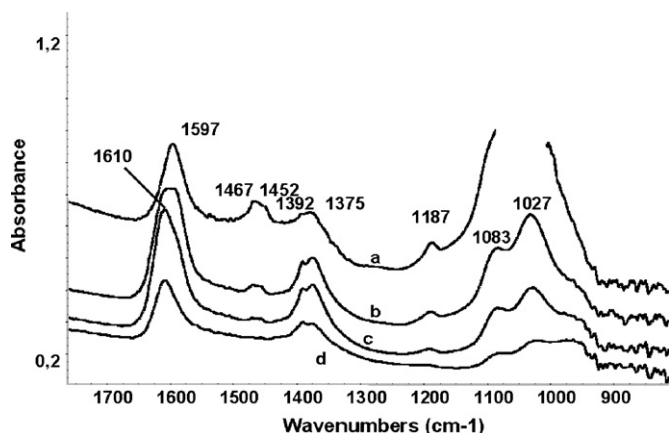


Fig. 6. FT-IR spectra of the adsorbed species formed upon adsorption on the catalyst, previously reduced in hydrogen at  $450\text{ }^{\circ}\text{C}$ , put into contact with water vapour and outgassed at  $250\text{ }^{\circ}\text{C}$ , of methanol 10 Torr at  $250\text{ }^{\circ}\text{C}$ ; in contact with the methanol vapour (a) and after outgassing at  $250\text{ }^{\circ}\text{C}$  (b),  $300\text{ }^{\circ}\text{C}$  (c), and  $350\text{ }^{\circ}\text{C}$  (d).

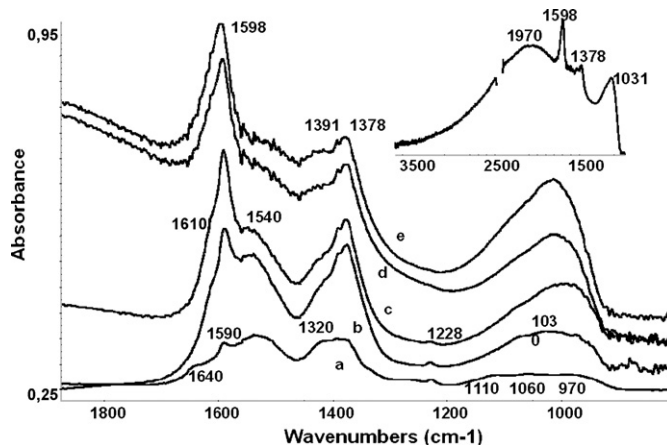


Fig. 7. FT-IR spectra of the adsorbed species formed upon adsorption on the catalyst, previously reduced in hydrogen at  $450\text{ }^{\circ}\text{C}$  and outgassed at  $450\text{ }^{\circ}\text{C}$ , of the mixture  $\text{CO}_2 + \text{H}_2$  at  $250\text{ }^{\circ}\text{C}$  upon increasing contact times (a) 10 min, (b) 20 min, (c) 40 min, (d) 60 min and (e) 90 min.

### 3.6. IR study of the reactivity toward $\text{CO}_2 + \text{H}_2$ mixture

The contact of the catalyst at  $250\text{ }^{\circ}\text{C}$  with the mixture  $\text{CO}_2 + \text{H}_2$  has also been investigated on a reduced sample. This contact (Fig. 7) causes the progressive growth of absorption bands due to carbonates ( $1540$ ,  $1320\text{ cm}^{-1}$ ) and bicarbonates ( $1640$ , ca.  $1400$ ,  $1228\text{ cm}^{-1}$ ) first, and to formate ions later ( $1598$ ,  $1393$  and  $1378\text{ cm}^{-1}$ ). It seems clear that the bands of formates form at the expense of those of carbonates and bicarbonates. Correspondingly, a further broad absorption grows with the most prominent maximum near  $1030\text{ cm}^{-1}$ . The position of this absorption is similar to that of some surface methoxy groups and also to that observed for hydrogen-reduced sample possibly associated to adsorbed hydrogen. A very broad absorption centered near  $2000\text{ cm}^{-1}$  also progressively grows (see the inset in Fig. 7), assigned to massive catalyst reduction, associated to an overall decrease of the light transmission by the sample.

These data agree with the very likely main mechanism of methanol synthesis over Cu–Zn–Al catalysts where  $\text{CO}_2$  is considered to be the actual reactant and, according to most authors [32], the mechanism is via carbonates–formates–methoxides.

### 3.7. IR study of low temperature CO adsorption

Low temperature CO adsorption is applied to characterize the surface of metal and oxide catalysts [33]. In Fig. 8a the IR spectrum of CO adsorbed at low temperature ( $-140\text{ }^{\circ}\text{C}$ ) on the reduced catalyst is reported. The main maximum is found at  $2150\text{ cm}^{-1}$ , with smaller maxima at  $2176$  and  $2120\text{ cm}^{-1}$ , and an evident tail both towards lower and higher frequencies. The lower frequency component at  $2120\text{ cm}^{-1}$  is formed at the highest coverages and has a complex behaviour. Its maximum shifts to higher frequencies, towards  $2130\text{ cm}^{-1}$ , and decreases in intensity by outgassing, but at higher temperatures,  $-70$ –( $-40$ )  $^{\circ}\text{C}$  the band broadens and displaces to lower frequencies again, to  $2115\text{ cm}^{-1}$ . The position and stability of this band strongly indicates that it is mainly due to the carbonyls of  $\text{Cu}^+$  ions or of small clusters of zerovalent copper. It is in

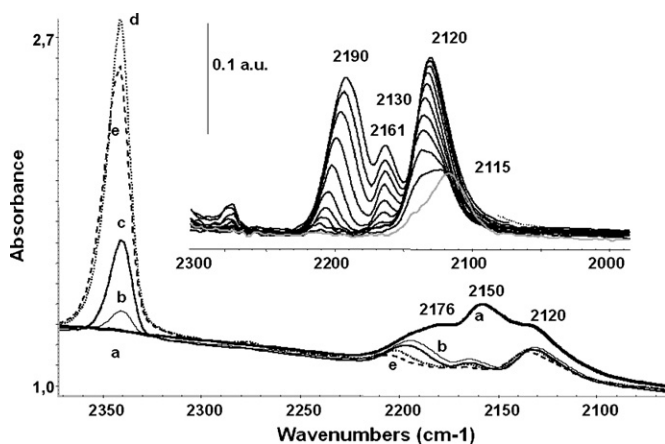


Fig. 8. FT-IR spectra of the adsorbed species formed upon adsorption of CO over the pre-reduced catalyst at  $-140^{\circ}\text{C}$  (a) and desorption at  $-140^{\circ}\text{C}$  (b),  $-130^{\circ}\text{C}$  (c),  $-100^{\circ}\text{C}$  (d) and  $-90^{\circ}\text{C}$  (e). In the inset, outgassing at increasing temperature ( $10^{\circ}\text{C}$  steps) from  $-140$ –( $-40$ )  $^{\circ}\text{C}$ .

fact well known that carbonyls on clean massive Cu metal are very weakly adsorbed and usually responsible for absorptions below  $2100$ – $2070\text{ cm}^{-1}$  [34–37]. It cannot be excluded that such species exist at the lowest temperatures and are responsible for the tail at lower frequency of this band. However, Cu metal particles may also present variable morphologies [38]. CO stretching frequencies above  $2100\text{ cm}^{-1}$  have also been reported for CO adsorbed on Cu small clusters and on copper particles containing on-top oxygen atoms [39].

Upon outgassing during warming the band at  $2150\text{ cm}^{-1}$  tends to disappear fast, showing that it is due, at least in part, to a very weakly adsorbed species, possibly physisorbed on the surface hydroxyl groups. However a component now at  $2161\text{ cm}^{-1}$  persists under low temperature outgassing. This feature can be assigned to CO adsorbed either on  $\text{Zn}^{2+}$  or on  $\text{Cu}^{2+}$  ions, although the assignment of at least part of this band to the higher frequency component of the CO stretching of  $\text{Cu}^{+}$  dicarbonyls is also possible, in agreement with Kannan et al. [40]. The lower frequency component of the CO stretching of  $\text{Cu}^{+}$  dicarbonyls is possibly near  $2100\text{ cm}^{-1}$ , at the lower frequency side of the main band.

The highest frequency band decreases less in intensity and shifts from  $2176$  to  $2204\text{ cm}^{-1}$  by decreasing coverage. Its position and its behaviour agrees with an assignment to CO adsorbed on  $\text{Al}^{3+}$  cations.

To discuss the bands due to adsorbed CO we have also to take into account that during CO desorption at  $-130$ –( $-100$ )  $^{\circ}\text{C}$  a strong absorption is formed and grows at  $2340\text{ cm}^{-1}$  certainly due to adsorbed  $\text{CO}_2$  (Fig. 7). By further warming upon outgassing the band decreases in intensity down to disappear at  $-40^{\circ}\text{C}$ . In these conditions, however, a shoulder forms and disappears at  $2355\text{ cm}^{-1}$ . The last components can be confidently assigned to  $\text{CO}_2$  adsorbed on  $\text{Al}^{3+}$  ions [41].

The formation, at so low a temperature, of adsorbed  $\text{CO}_2$  is certainly due to the existence of very active oxidizing sites, in spite of the reduction pre-treatment. According to previous studies [42,43],  $\text{Cu}^{2+}$  is very active in the low temperature oxidation of CO. We consequently conclude that at least part of

the band at  $2160\text{ cm}^{-1}$  is due to  $\text{Cu}^{2+}$  carbonyls that convert into  $\text{CO}_2$  complexes of  $\text{Cu}^{+}$  or  $\text{Cu}^0$ . Part of adsorbed CO jumps to the new reduced centers and this is at the origin of the sudden downwards shift of the band of adsorbed CO observed after the desorption of  $\text{CO}_2$ , which is found in the gas-phase spectra. Part of  $\text{CO}_2$  during desorption readsorbs over the stronger Lewis acidic  $\text{Al}^{3+}$  ions.

The analysis of the region  $2000$ – $1100\text{ cm}^{-1}$  does not show any evidence of the formation of formate ions nor of bicarbonate species. Very weak features at  $1600$  and  $1300\text{ cm}^{-1}$  show the formation of traces of carbonate ions.

These data show that the oxidation of CO to  $\text{CO}_2$  is a very fast reaction over Cu–Zn–Al catalysts, occurring even well below room temperature. The product of this oxidation is adsorbed  $\text{CO}_2$ . It is also relevant to note that the molecular adsorption of  $\text{CO}_2$  is weaker than the molecular adsorption of CO over  $\text{Cu}^{+}$  ions. Finally, it is also evident that desorption of  $\text{CO}_2$  may occur even without any formation of carbonate species. The formation of carbonate species is evidently an activated process.

### 3.8. IR study of high temperature CO adsorption

In Fig. 9 the spectra observed after contact of the reduced and rehydrated catalyst with CO at different temperatures are reported. After contact at r.t. the strong band, assigned (in agreement with the previous low temperature adsorption data) mostly to  $\text{Cu}^{+}$  carbonyls, is found at  $2113\text{ cm}^{-1}$ . By increasing the contact temperature the maximum of this band shifts progressively up to  $2120\text{ cm}^{-1}$  at  $300^{\circ}\text{C}$ .

Additionally, medium intensity sharp bands grow after contact at  $200^{\circ}\text{C}$  at  $1592$  and  $1374\text{ cm}^{-1}$ , assigned to formate ions. These bands are still present, even more intense, after contact at  $300^{\circ}\text{C}$ , but they are now superimposed to a broader absorption (main maxima near  $1550$  and  $1430\text{ cm}^{-1}$ ), attributed to carbonate ions. The analysis of the gas phase shows that carbon dioxide is formed from CO starting from  $100^{\circ}\text{C}$ . After contact at  $400^{\circ}\text{C}$  the band of adsorbed CO is no more observed and a very strong

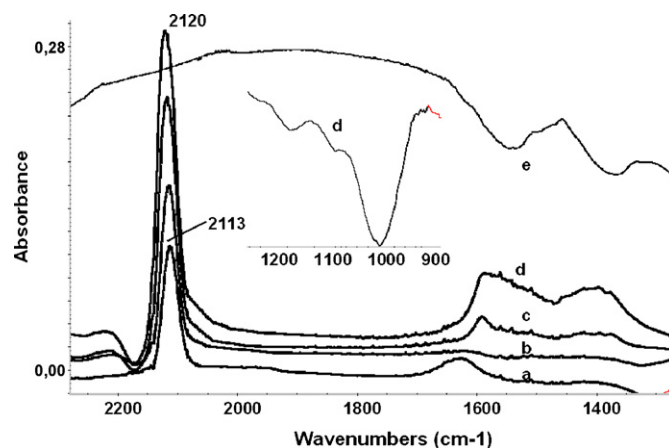


Fig. 9. FT-IR spectra of the adsorbed species formed upon interaction of CO with a pre-reduced and hydrated catalyst at r.t. (a),  $100^{\circ}\text{C}$  (b),  $200^{\circ}\text{C}$  (c),  $300^{\circ}\text{C}$  (d) and  $400^{\circ}\text{C}$  (e). The inset: negative band possibly due to the perturbation of surface metal-oxygen bonds.

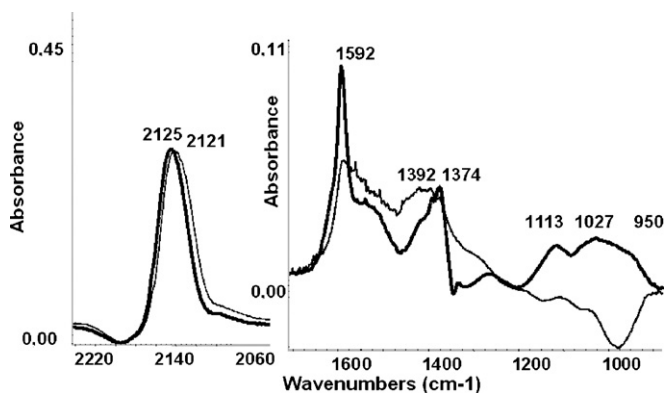


Fig. 10. FT-IR spectra of the adsorbed species formed upon interaction of CO at 250 °C with a pre-reduced catalyst (bold line) and a catalyst previously pre-reduced and hydrated (thin line).

and broad absorption is now evident, centered near 2000  $\text{cm}^{-1}$ . This absorption has been attributed to a full reduction of the catalyst.

In Fig. 10 the spectra of CO adsorbed at 250 °C on a sample which has been previously reduced and on a sample which has been previously reduced and hydrated are compared. In the case of the simply reduced catalyst the bands of formate ions are apparently much sharper and stronger, in part because the bands of carbonate ions are less intense, if present at all. Moreover, the CO stretching of the surface carbonyls is a little shifted at higher frequencies (2125  $\text{cm}^{-1}$ ), with respect to what observed with the sample which has been also hydrated. This suggests that hydration could increase the coordination sphere of  $\text{Cu}^+$  ions so making them more electron dense, so increasing the backdonation to the CO antibonding orbitals. Finally, it is worth noting that a positive absorption is found in the region below 1200  $\text{cm}^{-1}$ , with two distinct maxima at 1113 and 1026  $\text{cm}^{-1}$ , and a component at 950  $\text{cm}^{-1}$ . The components at 1026 and 950  $\text{cm}^{-1}$  are similar to those observed upon methanol adsorption on oxidized and hydrated catalyst. These absorptions are associated to C–O stretchings of surface methoxy groups. This shows that, under these conditions, the reduced catalyst provides some hydrogen to CO giving rise to most steps of methanol synthesis. The component at 1113  $\text{cm}^{-1}$  may be associated to the CO stretching of a dioxymethylene species [44,45], which may be an intermediate in methoxy groups formation.

The adsorption of CO on the reduced and hydrated catalyst gives rise to smaller bands of formates and stronger absorption associated to carbonates, as well as a negative absorption in the region near 1000  $\text{cm}^{-1}$ . This absorption is frequently found after adsorption of different species on aluminas and different aluminates [46], and has been assigned to the perturbation of surface metal oxygen bonds of oxides by adsorbed species. This feature is not observed if vibrational modes of adsorbed species are superimposed on it, like in all previous experiments reported here. The spectra reported in Fig. 10 confirm that the surface of the hydrogen-reduced sample is strongly reducing (giving rise to methoxy groups from CO), whereas that of the rehydrated sample is more oxidizing (giving rise to carbonates and  $\text{CO}_2$  in the gas phase).

These data show that the surface pretreated in water is more oxidizing than that simply reduced. While in both cases formate species are formed by CO reaction likely with hydroxy groups, the ratio between carbonates and formates is by far higher on the prehydrated surface.

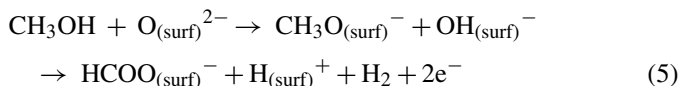
## 4. Discussion

### 4.1. Methanol (oxidative) steam reforming

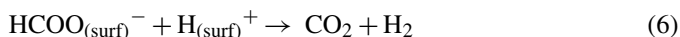
The experiments described in this paper give indications concerning the possible mechanisms of methanol steam reforming and related reactions over  $\text{Cu-ZnO-Al}_2\text{O}_3$  catalyst. The IR data concerning the adsorption and conversion of methanol provide evidence for the mechanism involving surface methoxides and formate species, in agreement with the previous literature. Our data also show that at relatively low temperature the main C-containing product of methanol decomposition is  $\text{CO}_2$ , while at higher temperatures CO is mostly formed, over an unreduced catalyst.

Just the same result is obtained over a catalyst that has been pre-reduced in hydrogen and then treated with water vapour at 250 °C. Instead, the interaction of a simply reduced catalyst with methanol is different. The intensities of the bands relative to the adsorbed species is greatly decreased by reduction and re-increased by hydration. This is an evidence of the ability of water vapour to oxidize reduced copper centers, producing copper ions and hydrogen gas. Dissociative adsorption of methanol should mostly occur on the dispersed and oxidized copper sites present on at least partially oxidized surfaces.

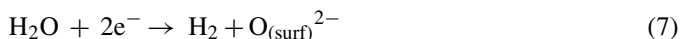
Methoxides over these surfaces first transform into formates. It is worth noting that this is an oxidation reaction and consequently implies a reduction of the previously oxidized surface sites:



The successive decomposition of formates occurs, giving rise to evolution of  $\text{CO}_2$  at relatively low temperatures, while at higher temperatures CO is evolved. The decomposition of formates to  $\text{CO}_2$  does not imply any change in the catalyst oxidation state:



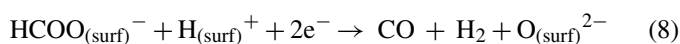
Thus, the sum of reactions (5) and (6) is, as far as the catalyst is concerned, a reduction semireaction. Water is in fact an oxidizing co-reactant needed to convert methanol to  $\text{CO}_2$  and hydrogen (i.e. making steam reforming) through the following reaction:



MSR, reaction (4), occurring through methoxide and formate species, should consequently be the sum of reactions (5) + (6) + (7). Our data and their interpretation allow us to conclude that MSR is a redox reaction with methanol acting as a

reductant for the catalyst and water acting as an oxidant for the reduced catalyst.

Formate species may also decompose giving rise to gas-phase CO:



Thus, the question arises whether the primary gas phase product upon methanol steam reforming is CO (through reaction (8)), which is later converted to CO<sub>2</sub> through the water gas shift reaction (2), or CO<sub>2</sub> is directly formed by formates decomposition (through reaction (6)). It has already been discussed that the production of CO upon MSR is much lower and that of CO<sub>2</sub> much higher than those forecast on the basis of the WGS equilibrium. This implies that CO<sub>2</sub> is the primary gaseous product of MSR, CO gas being possibly produced by the reverse-WGS reaction:



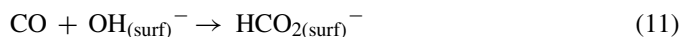
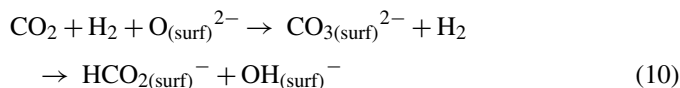
or by a secondary reaction path.

However, it is not excluded that CO is formed in large amounts by reaction (8) but remains adsorbed on the surface. We have in fact shown that CO is adsorbed strongly and very easily and rapidly converted into CO<sub>2</sub> over oxidized copper centers. This seems to be the most likely mechanism on the basis of our data. Our data seem also to exclude that carbonate species may play an important role in the MSR reaction. In fact, CO<sub>2</sub>, just after being formed either by direct formate decomposition or by CO oxidation, may either leave rapidly the surface at low temperature, or reversibly adsorb in the form of carbonates. In Scheme 1 a mechanism for the MSR reaction is proposed, which is actually the sum of reactions (5) + (6) + (7), with the intermediate formation of adsorbed CO which is converted to CO<sub>2</sub> over oxidized copper centers.

The presence of oxygen in the oxidative steam reforming reaction obviously also allows relatively high oxidation state of copper centers so finally favouring the CO oxidation step.

#### 4.2. Water gas shift equilibrium

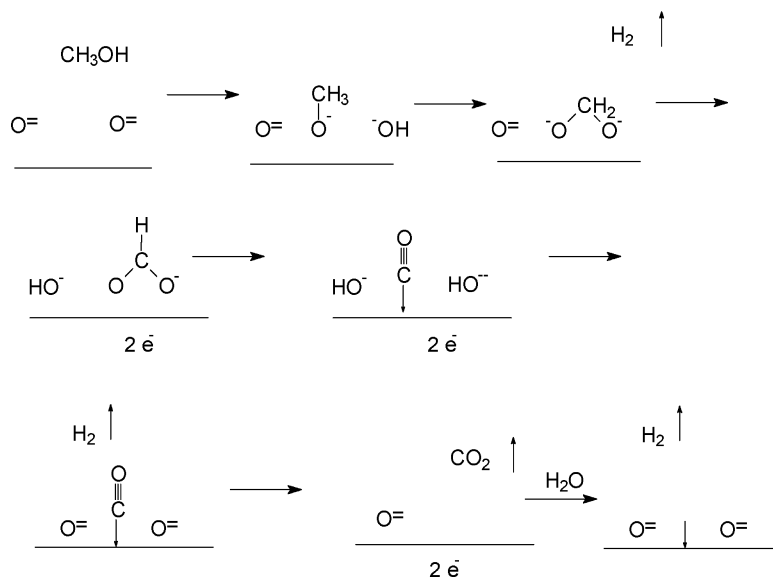
Our data indicate that very likely both the redox mechanism and the associative mechanism through formate species are active for the WGS equilibrium. In fact we confirm that formate species are actually formed both from CO on the hydrated surface and from CO<sub>2</sub> + H<sub>2</sub>, in agreement with a previous IR study [32].



On the other hand, the effect of water vapour in oxidizing the surface is quite evident too, and the high velocity of CO oxidation is also well proved. We suggest that the associative mechanism is likely predominant at low temperature where the equilibrium favours the WGS reaction, while the associative mechanism is more likely at higher temperature, where the reverse-WGS is less unfavored. In this case in fact to activate CO<sub>2</sub> its strong adsorption in the form of carbonates is possibly needed and the further conversion to formates likely becomes necessary.

This conclusion does not conflict with that reported by Fujita et al. [47] that support the redox mechanism for the reverse-WGS reaction over Cu/ZnO. These authors work at very low temperature (165 °C) even if at this temperature the reverse WGS is unfavored ( $\Delta G^\circ$  for the WGS equilibrium is 0 at 830 °C).

Our conclusion is just the opposite of the conclusion of Callaghan et al. [48] who studied the WGS reaction over Cu(1 1 1) monocrystal surface by a theoretical approach and, by comparison, with experimental data. These authors concluded that the associative mechanism is predominant at low temperatures while the redox one is predominant at high temperature. We believe, however, that the real catalyst for this reduction is not metallic copper. The support on which oxidized copper ions



Scheme 1. Proposed mechanism for the MSR reaction over Cu–Zn–Al catalyst.



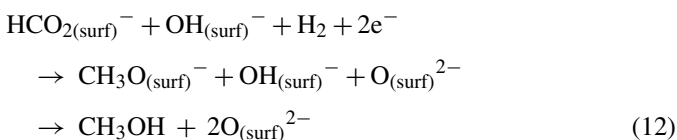
may disperse may play a relevant role and may change very much the stability and the nature of the adsorbed species.

The inhibiting effect of the product CO<sub>2</sub>, emphasized by Trimm [4], on the WGS reaction may be just explained by the strong adsorption of CO<sub>2</sub> in the form of carbonates.

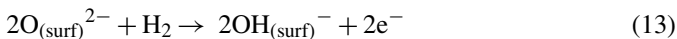
#### 4.3. Methanol synthesis and decomposition

The aim of this work was not to study the mechanism of methanol synthesis. In any case, our data do not disagree with those previously reported on similar catalysts [41,49,50]. Our data show that methoxy groups are formed both by reaction of CO<sub>2</sub> + H<sub>2</sub> mixture and by adsorption of CO over a reduced surface where adsorbed hydrogen is present, at 250 °C. Formate species are likely intermediates in both cases.

Formate species are later hydrogenated to methoxy groups and to methanol,



It seems interesting to remark that the synthesis of methanol from CO and hydrogen, if occurring through formate ions, implies the reduction of the catalyst by hydrogen:



to produce the sequence of reactions (11) + (12) + (13). In practice, the catalyst also undergoes redox cycles.

Methanol decomposition to CO and hydrogen is just the reverse of methanol synthesis from CO, and likely occurs through the sequence of reactions (5) + (8). We believe that the reaction of methanol decomposition (due to the absence of any oxidizing species among reactants and products) occurs on a highly reduced catalyst, where copper metal is in fact the real catalyst. This agrees with recent data for methanol synthesis, where it has been found that the more reducing the gas the more active the catalyst, and the more dispersed the zerovalent copper particles [38,51]. For this reason the formate species convert to CO through reaction (8). The formation of small amounts of CO upon MSR, in our case, may be just related to the higher reduction degree of the catalyst at high-temperatures, that tends to favour step (8) or to limit CO oxidation to CO<sub>2</sub>. So, it is more likely due to a parallel path than to the successive reverse-WGS reaction over the main product CO<sub>2</sub>.

## 5. Conclusions

IR spectroscopy experiments of adsorption and coadsorption of methanol, water, CO, CO<sub>2</sub> and hydrogen allowed us to propose a mechanism for the methanol steam reforming and oxidative steam reforming and to add some consideration on the mechanisms of the water gas shift equilibrium and of methanol synthesis and decomposition.

Our conclusions are that methanol steam reforming occurs over Cu–Zn–Al catalysts via the adsorbed methoxy

groups/adsorbed formate ions/adsorbed CO/CO<sub>2</sub> sequence. Water oxidizes part of Cu species and forms hydroxyl groups. Our data also support the redox mechanism for WGS at low temperature. These reactions probably occur with partially oxidized copper centers. Methanol decomposition and its synthesis from pure CO + H<sub>2</sub>, instead, occur likely over fully reduced copper catalysts.

## Acknowledgement

The authors acknowledge funding from MIUR PRIN.

## References

- [1] I. Wender, Fuel Proc. Technol. 48 (1996) 189.
- [2] M.V. Twigg, Catalyst Handbook, 2nd ed., 1989, pp. 283–339.
- [3] P.R. Davies, F.F. Snowden, G.W. Bridger, D.O. Huges, D.W. Young, US Patent 1,010,871 (1966).
- [4] D.L. Trimm, Appl. Catal. A: Gen. 296 (2005) 1.
- [5] H. Tøpsoe, brochure “Package hydrogen plants” available in the web: <http://www.topsoe.com>.
- [6] Gulf Pub. Co., Hydrocarbon Processing: Gas Processes, 2004.
- [7] B.S. Rasmussen, P.E. Højlund Nielsen, J. Villadsen, J.B. Hansen, Preparation of catalysts IV, in: B. Delmon, P. Grange, P.A. Jacobs, G. Poncelet (Eds.), Studies in Surface Science and Catalysis, vol. 31, 1987, p. 785.
- [8] C.V. Ovesen, B.S. Clausen, B.S. Hammershøi, G. Steffensen, T. Askgaard, I. Chorkendorff, J.K. Nørskov, P.B. Rasmussen, P. Stoltze, P. Taylor, J. Catal. 158 (1996) 170.
- [9] Ju.Y. Won, H.K. Jun, M.K. Jeon, S.I. Woo, Catal. Today 111 (2006) 158.
- [10] P. Pfeifer, K. Schubert, G. Emig, Appl. Catal. A: Gen. 286 (2005) 175.
- [11] J.K. Lee, J.B. Ko, D.H. Kim, Appl. Catal. A: Gen. 278 (2004) 25.
- [12] D.G. Löffler, S.D. McDermott, C.N. Renn, J. Power Sources 114 (2003) 15.
- [13] M. Turco, G. Bagnasco, U. Costantino, F. Marmottini, T. Montanari, G. Ramis, G. Busca, J. Catal. 228 (2004) 43.
- [14] M. Turco, G. Bagnasco, U. Costantino, F. Marmottini, T. Montanari, G. Ramis, G. Busca, Chem. Eng. Trans. 6 (2005) 19.
- [15] G. Busca, U. Costantino, F. Marmottini, T. Montanari, P. Patrono, F. Pinzari, G. Ramis, Appl. Catal. A: Gen. 310 (2006) 70.
- [16] Y. Choi, H.G. Stenger, J. Power Sources 124 (2003) 432.
- [17] G.C. Chinchin, M.S. Spencer, Catal. Today 10 (1991) 293.
- [18] Y. Choi, H.G. Stenger, J. Power Sources 142 (2005) 81.
- [19] H. Purnama, T. Ressler, R.E. Jentoft, H. Soerijanto, R. Schlögl, R. Schomäcker, Appl. Catal. A: Gen. 259 (2004) 83.
- [20] J. Agrell, H. Birgeron, M. Boutonnet, J. Power Sources 106 (2002) 249.
- [21] J.K. Lee, J.B. Ko, D.H. Kim, Appl. Catal. A: Gen. 278 (2004) 25–35.
- [22] B.A. Peppely, J.C. Amphlett, L.M. Kearns, R.F. Mann, Appl. Catal. A: Gen. 179 (1999) 31.
- [23] K. Klier, V. Chatikavanij, R.G. Herman, G.W. Simmons, J. Catal. 74 (1982) 343.
- [24] X. Huang, L. Ma, M.S. Wainwright, Appl. Catal. A: Gen. 257 (2004) 235.
- [25] U. Costantino, F. Marmottini, M. Sisani, T. Montanari, G. Ramis, G. Busca, M. Turco, G. Bagnasco, Solid State Ionics 176 (2005) 2917.
- [26] V. Rives (Ed.), Layered Double Hydroxides: Present and Future, Nove Sci. Pub., New York, 2001.
- [27] G. Busca, A. Vaccari, J. Chem. Soc. Chem. Commun. (1988) 788.
- [28] G. Busca, P.F. Rossi, V. Lorenzelli, M. Benaissa, J. Travert, J.C. Lavalley, J. Phys. Chem. 89 (1985) 5433.
- [29] A. Riva, F. Trifirò, A. Vaccari, L. Mintchev, G. Busca, J. Chem. Soc., Faraday Trans. 184 (1988) 1423.
- [30] M.A. Chester, E.M. McCash, Spectrochim. Acta A 43 (1987) 1625.
- [31] G. Busca, J. Lamotte, J.C. Lavalley, V. Lorenzelli, J. Am. Chem. Soc. 109 (1987) 5197.
- [32] F. Le Peltier, P. Chaumette, J. Saussey, M.M. Bettahar, J.C. Lavalley, J. Mol. Catal. A: Chem. 132 (1998) 91.

- [33] K.I. Hadjiivanov, G.N. Vayssilov, *Adv. Catal.* 47 (2002) 307.
- [34] J. Pritchard, T. Catterick, R.K. Gupta, *Surf. Sci.* 53 (1975).
- [35] K. Horn, J. Pritchard, *Surf. Sci.* 55 (1976) 706.
- [36] K. Horn, M. Hussain, J. Pritchard, *Surf. Sci.* 63 (1977) 244.
- [37] T. Wadayama, Y. Sasaki, K. Shiomitsu, A. Hatta, *Surf. Sci.* 592 (2005) 72.
- [38] J.-D. Grunwaldt, A.M. Molenbroek, N.-Y. Topsøe, H. Topsøe, B.S. Clausen, *J. Catal.* 1948 (2000) 452.
- [39] J. Greeley, A.A. Gokhale, J. Kreuser, J.A. Dumesic, H. Topsøe, N.-Y. Topsøe, M. Mavrikaki, *J. Catal.* 213 (2003) 63.
- [40] S. Kannan, Tz. Venkov, K. Hadjiivanov, H. Knözinger, *Langmuir* 20 (2004) 730.
- [41] C. Morterra, G. Magnacca, *Catal. Today* 27 (1996) 497.
- [42] G. Busca, *J. Mol. Catal.* 43 (1987) 225.
- [43] J.M. Gallardo Amores, V. Sanchez Escibano, G. Busca, V. Lorenzelli, *J. Mater. Chem.* 4 (1994) 965.
- [44] H. Idriss, J.P. Hindermann, R. Kieffer, A. Kiennemann, A. Vallet, C. Chauvin, J.C. Lavalley, P. Chaumette, *J. Mol. Catal.* 42 (1987) 205.
- [45] G. Busca, J. Lamotte, J.C. Lavalley, V. Lorenzelli, *J. Am. Chem. Soc.* 109 (1987) 5197.
- [46] G. Busca, V. Lorenzelli, V. Sanchez Escibano, R. Guidetti, *J. Catal.* 131 (1991) 167.
- [47] S. Fujita, M. Usui, N. Takezawa, *J. Catal.* 134 (1992) 220.
- [48] C. Callaghan, I. Fishtik, R. Datta, M. Carpenter, M. Chmielewski, A. Lugo, *Surf. Sci.* 541 (2003) 21.
- [49] J. Saussey, J.C. Lavalley, *J. Mol. Catal.* 50 (1989) 343.
- [50] F. Le Peltier, P. Chaumette, J. Saussey, M.M. Bettahar, J.C. Lavalley, *J. Mol. Catal. A: Chem.* 122 (1997) 131.
- [51] N.-Y. Topsøe, H. Topsøe, *J. Mol. Catal. A: Chem.* 141 (1999) 95.